Title

Food glycomics: Dealing with unexpected degradation of oligosaccharides during sample preparation and analysis.

Journal

Journal of food and drug analysis, 30(1)

ISSN

1021-9498

Authors

Huang, Yu-Ping
Robinson, Randall C
Barile, Daniela

Publication Date

2022-03-01

DOI

10.38212/2224-6614.3393

Peer reviewed

Journal of Food and Drug Analysis

Volume 30 | Issue 1 Article 6

2022

Food glycomics: Dealing with unexpected degradation of oligosaccharides during sample preparation and analysis

ORIGINAL ARTICLE

Food glycomics: Dealing with unexpected degradation of oligosaccharides during sample preparation and analysis

Yu-Ping Huang [a], Randall C. Robinson [a], Daniela Barile [a,b,*]

[a] Department of Food Science and Technology, University of California-Davis, Davis, CA, USA
[b] Foods for Health Institute, University of California-Davis, Davis, CA, USA

Abstract

This study reveals that unexpected degradation of food oligosaccharides can occur during conventional glycomics workflows, including sample preparation and analysis by liquid chromatography-mass spectrometry (LC-MS). With the present investigation, we aim to alert the scientific community of the susceptibility of specific glycosidic linkages to degradation induced by heat and acid. Key standard oligosaccharides representing the major types found in foods (3′-sialyllactose and 6′-sialyl-N-acetyllactosamine for milk, raffinose and stachyose for legumes) were selected as model systems and underwent each of the following treatments independently: (1) labeled with the derivatizing agent 1-aminopyrene-3,6,8-trisulfonic (APTS) (followed by analysis with a capillary electrophoresis system coupled with a fluorescence detector), (2) dried from an acetonitrile-water mixture containing 0.1% trifluoroacetic acid, and (3) injected into an LC-MS system. We demonstrated that both raffinose and stachyose degraded during APTS-labeling by the acid in the labeling reagents. We also discovered that during centrifugal evaporation at 37 °C, all of the four nonderivatized oligosaccharides tested were partially degraded. Additionally, when the LC-MS eluent contained 0.1% formic acid, 3′-sialyllactose, raffinose, and stachyose underwent extensive in-source fragmentation during analysis. Lastly, we identified a simple strategy that can reduce the probability of incorrect oligosaccharide identification resulting from extensive in-source fragmentation.

Keywords: In-source fragmentation, Oligosaccharide degradation, Raffinose-family oligosaccharides, Reductive amination, Sialylated oligosaccharides

1. Introduction

Oligosaccharides (OS) are carbohydrates composed of 3−20 monosaccharide moieties. They naturally exist in free form in foods, such as milk, legumes, honey, and vegetables, and can be generated through processing techniques, including enzymatic synthesis, depolymerization of polysaccharides, and enzymatic release from glycoproteins [1,2]. Glycosyltransferases are commonly adopted for OS synthesis using simple sugars as substrates, such as in the production of galactooligosaccharides and fructooligosaccharides [3]. Polysaccharide depolymerization can be fulfilled enzymatically, chemically, or physically, as seen in the production of fructooligosaccharides from inulin and xylooligosaccharides from xylan [4−7]. N-Glycosylation is a co/post-translational modification. Glycoproteins with N-glycosylation can release N-glycans via enzymatic treatment using specific enzymes and have become an emerging source of OS [2,8].

Some OS that are resistant to digestion can be utilized by commensal bacteria in the human gut and selectively stimulate the growth of beneficial intestinal bacteria, including species from the genera *Bifidobacterium*, *Lactobacillus*, and *Eubacterium*. In turn, they can render health benefits to the host, such as increasing mineral absorption, regulating blood lipid and blood glucose, reducing the risk of colon cancer, and modulating immune

Received 19 September 2021; revised 11 November 2021; accepted 22 November 2021.
Available online 15 March 2022.

* Corresponding author at: Department of Food Science and Technology, University of California-Davis, Davis, CA, USA. Fax: +530 752 4759.
E-mail address: dbarile@ucdavis.edu (D. Barile).

https://doi.org/10.38212/2224-6614.3393

function [9]. The fermentability of different types of OS that originate from various sources or are produced via different processing techniques may vary and depends on whether the intestinal bacteria can generate the corresponding glycolytic enzymes to cleave the specific glycosidic linkages and whether the bacteria can further utilize the released monosaccharides. Therefore, collecting detailed information on OS structures, including monosaccharide units, degree of polymerization (DP), and types of glycosidic linkages, is critical when studying and predicting their fermentability, prebiotic properties, and structure-function relationships.

Acids are frequently used in the processing and analysis of food carbohydrates. Several of these techniques are based on the hydrolysis of glycosidic linkages in carbohydrates. For example, hydrolysis using hydrochloric or sulfuric acid at elevated temperatures (above 60 °C) is used for producing oligosaccharides with potential prebiotic property from polysaccharides on a large scale [10]. Dilute hydrochloric or sulfuric acid is also used for treating starch granules to modify starch structure and functionality [11]. Acid hydrolysis is also a crucial step in monosaccharide composition analysis for breaking down carbohydrates with various DP into constituent monosaccharides using sulfuric or trifluoroacetic acid (TFA) [12,13]. Dilute acids can serve other purposes in the analysis of food carbohydrates that are unrelated to OS hydrolysis, such as functioning as an electronic modifier or pH modifier in solid-phase extraction and liquid chromatography [14]. Furthermore, as carbohydrates are invisible to UV-spectroscopy and fluorescence detectors, labeling OS via reductive amination is widely used to conjugate a chromophore or fluorophore to OS, and acids are necessary to catalyze the reaction [15,16]. One potential issue associated with this strategy is that the acids may partially detach sialic acid monosaccharides from sialylated OS, causing alterations in the structure and function as well as distorting analytical results [17–19]. The labeling step may be circumvented through analyzing native OS with analytical techniques that do not rely on the detection of chromophores or fluorophores, such as high-performance anion-exchange chromatography with pulsed amperometric detection (HPAEC-PAD), high-performance liquid chromatography (HPLC) coupled to refractive index or evaporative light scattering detection, and mass spectrometry. Nonetheless, some steps in the OS analytical workflows may still involve the use of acids. Due to acids' tendency of causing hydrolysis of glycosidic linkages, it is possible that OS analysis steps where acids are necessarily used may result in certain degradation of susceptible OS.

The present work studied the degradation of OS standards during three critical steps in common glycomics analysis workflows, including APTS labeling, solvent evaporation in the presence of TFA, and LC-MS analysis, to examine the susceptibility of specific food OS to acid-induced degradation and inform about the potential problems of using acids in routine glycomic analysis. We also offer potential solutions to address the undesirable OS degradation and achieve unambiguous OS identification.

2. Materials and methods

2.1. Materials

Sucrose, raffinose pentahydrate, stachyose hydrate, fructose, glucose, invertase from baker's yeast, and TFA were purchased from MilliporeSigma (St. Louis, MO, USA). 3′-Sialyllactose (3′-SL) and 6′-sialyl-N-acetyllactosamine (6′-SLN) were obtained from V-Labs (now Dextra Laboratories Ltd., Reading, Berkshire, UK). Melibiose was obtained from TCI (Tokyo, Japan). Xylosyl-cellobiose (borohydride reduced) was purchased from Megazyme (Bray, Ireland). N-Glycans were released from an almond flour protein-rich extract by glycopeptidase A (MilliporeSigma).

2.2. APTS-labeling of OS and capillary electrophoresis

Glucose, fructose, sucrose, raffinose, stachyose, and melibiose standard solutions (1–2 μL) were transferred to 1.5-mL centrifuge tubes and dried in a centrifugal evaporator (MiVac Quattro, Genevac Ltd., Ipswitch, Suffolk, UK) at room temperature. APTS solution, reductant solution, and strong acid catalyst in a Prozyme GlykoPrep APTS labeling module (Agilent Technologies, Santa Clara, CA, USA) were mixed in the ratio of 1.2:1.2:3.0 (v/v/v). The dried carbohydrate standards were dissolved with 4.5 μL of the mixed labeling reagents and incubated at 65 °C for 1 h in a Thermomixer (Eppendorf North America, Hauppauge, NY, USA). Following incubation, the tubes were removed from the Thermomixer and were placed in a fume hood with the lid open for 20 min to dissipate any hydrogen cyanide formed during incubation. The samples were mixed with 200 μL of 85% acetonitrile (v/v) and cleaned up with a Gly-Q cartridge module (Agilent Technologies). After cleanup, the samples were diluted and analyzed by the Gly-Q Glycan Analysis System (Agilent Technologies). Brackets of

DP 2 and DP 15 (labeled with a non-APTS fluorophore; provided by Agilent Technologies) were added to each injection for aligning electropherograms by glucose units.

2.3. Solvent evaporation of OS standards in the presence or absence of TFA

OS standard solutions containing 1 μg of 6′-SLN, 3′-SL, or a mixture of raffinose and stachyose (1 μg each) were prepared in 40% acetonitrile in water (v/v) or 40% acetonitrile in water containing 0.1% TFA (v/v/v) with a total volume of 600 μL. The samples were dried by a centrifugal evaporator at room temperature (no heat applied; ~23–26 °C) or 37 °C.

2.4. Enzymatic treatment with invertase (EC 3.2.1.26) to confirm raffinose and stachyose degradation products

To verify the identities of degradation products generated from raffinose and stachyose during solvent evaporation in the presence of TFA, melibiose and manninotriose were enzymatically produced from raffinose and stachyose standards, respectively, to allow direct comparison with the observed degradation products in the evaporated samples. Invertase is a β-D-fructofuranosidase, which can specifically cleave fructose from raffinose and stachyose, and was chosen for this enzymatic treatment. Raffinose (60 μg of raffinose pentahydrate) and stachyose (80 μg of stachyose hydrate) standards were individually incubated with invertase (10 μg) for 10 min (pH 4.5, 50 °C, and 300 rpm) in a Thermomixer. After the incubation, the samples were heated in a boiling water bath for 5 min to inactivate the invertase. The inactivated enzymes were removed by solid-phase extraction by loading samples onto C18 cartridges (Discovery DSC-18, 100 mg, MilliporeSigma) preconditioned with 2 mL ACN followed by 2 mL water, and then washing the cartridges with 2 mL water to recover carbohydrates. The purified carbohydrates were then analyzed with LC-MS.

2.5. LC-MS analysis

LC-MS analysis was performed on an Agilent 6520 Accurate-Mass Q-TOF LC-MS with a Chip Cube interface equipped with an Agilent PGC-Chip II (porous graphitized carbon chip with a 40-nL enrichment column and a 75 μm × 43 mm analytical column). The capillary pump delivered 3% acetonitrile with 0.1% formic acid (v/v/v) at a flow rate of 4 μL min^{-1} and loaded samples onto the enrichment column. The injection volume was 2 μL for each sample. The nano pump delivered mobile phase composed of 3% acetonitrile with 0.1% formic acid (v/v/v) (solvent A) and 89.9% acetonitrile with 0.1% formic acid (v/v/v) (solvent B). The analytes were separated using the nano pump at a flow rate of 0.3 μL min^{-1} with 0% B from 0.0 − 2.0 min; 0–3% B from 2.0 to 3.0 min; 3–15% B from 3.0 to 15.0 min; 15–30% B from 15.0 to 16.5 min; 30–100% B from 16.5 to 18.5 min; 100% B 18.5–21.0 min. The mobile phase was switched to 100% A and equilibrated for 9 min before the next injection. The capillary voltage was varied between 1850—1940 V as needed to maintain a stable solvent spray. The drying gas was set at 350 °C with a flow rate of 5 L min^{-1}. When studying the effect of TFA on OS degradation, the dried samples were re-dissolved and diluted with nanopure water to a concentration corresponding to 10 μg mL^{-1} of the original OS and spiked with xylosyl-cellobiose at a concentration of 1 μg mL^{-1} as an internal standard. Peak areas of each analyte were integrated with MassHunter Qualitative Analysis software version B.07.00 (Agilent Technologies) after extracting the protonated molecules ($[M+H]^+$) and corresponding in-source fragment ions and aggregate ions as a merged extracted-ion chromatogram. Relative quantification was done by normalizing the peak area of analytes against the peak area of xylosyl-cellobiose to compensate for differences in ionization efficiency between runs. These values were then divided by the normalized peak area of the OS samples dried at room temperature in absence of TFA to obtain each OS abundance as a percentage. In a second round of experiments, 0.1% formic acid in the mobile phase was replaced with 5 mM ammonium acetate in an attempt to reduce the extent of in-source fragmentation through the formation of ammonium adducts. Tandem MS analysis was conducted using collision energies determined by the formula [collision energy (V) = 0.013 × m/z − 3.5].

3. Results and discussion

Two common workflows used in glycomic analysis and the steps at which OS degradation or fragmentation may arise are summarized in Fig. 1A and B. Caution is required when these steps are used in glycomic analysis in order to avoid incorrect interpretation of experimental data. Labeling of OS at their reducing end via reductive amination is commonly applied for glycomic analysis to enable or improve the separation and detection of carbohydrates [16,20–23]. Analysis of native (unlabeled) OS is often achieved by mass spectrometry to obtain

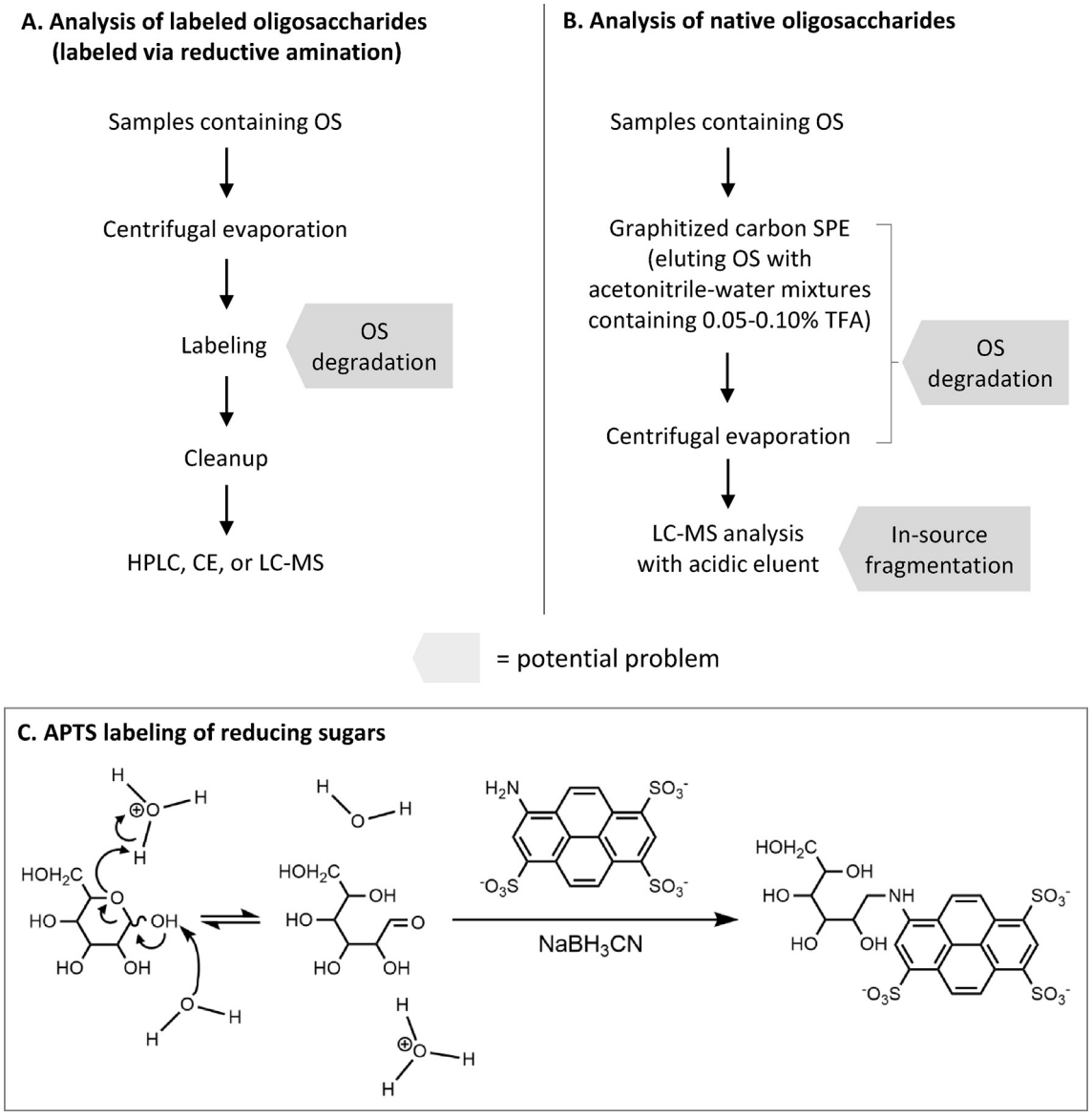

Fig. 1. Critical steps in conventional glycomic analysis workflows for labeled (A) and native (B) OS analysis, and APTS labeling reaction to reducing sugars, which are represented by a hexose in this figure (C). The critical steps leading to OS degradation or fragmentation evidenced in the current work are indicated by shaded arrows. CE: capillary electrophoresis.

molecular weights and compositional information, and is an important approach for both targeted and untargeted glycomics [24–26]. The following sections demonstrate and discuss the potential issues of these workflows.

3.1. Degradation of OS during APTS labeling

APTS labeling is one of the OS labeling methods utilizing reductive amination (Fig. 1A). To enable the reaction between OS and labeling reagents, a significant amount of acid is typically required to catalyze the hemiacetal ring-opening on the reducing end of OS (Fig. 1C). However, it is well known that acids may cause sialic acid monosaccharides to detach from sialylated OS at elevated temperatures (37–60 °C with various incubation times) [17–19]. Therefore, the labeling conditions usually need to be optimized for maximizing the labeling efficiency and minimizing undesirable degradation. In this study, we found that, in addition to the widely known partial degradation of sialylated OS [17–19], some non-reducing sugars might also be susceptible to such acidic labeling conditions. Surprisingly, after undergoing the APTS labeling, sucrose, raffinose, and stachyose displayed

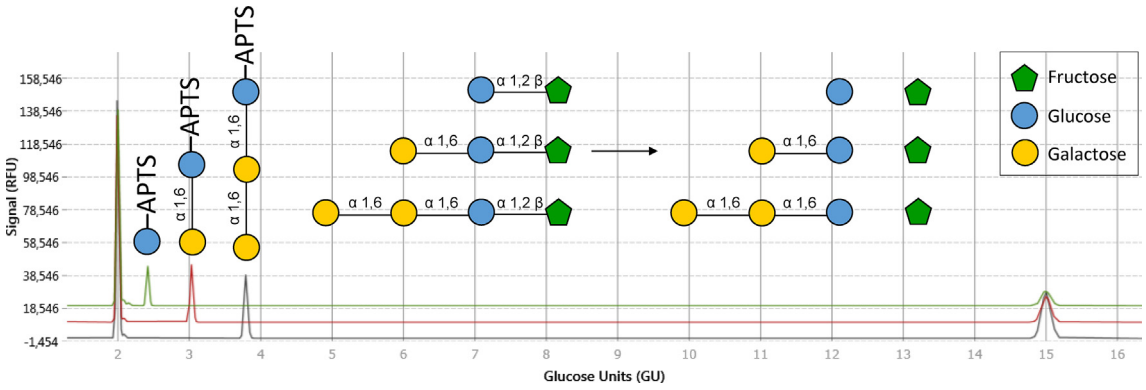

Fig. 2. Overlaid Gly-Q capillary electropherograms of degradation products of sucrose (top), raffinose (middle), and stachyose (bottom) following APTS labeling treatment at 65 °C for 1 h. Peaks at 2 and 15 glucose units (GU) are DP 2 and DP 15 brackets, respectively.

clear peaks at 2.4, 3.0, and 3.8 glucose units, respectively, on the CE electropherograms (Fig. 2). Because the labeling is based on the reaction between the primary amine of APTS and the aldehyde group on the reducing end of carbohydrates (Fig. 1C), non-reducing sugars, such as the three studied here, should neither react with APTS nor generate fluorescence signal after the APTS labeling step. The occurrence of the peaks shown in Fig. 2 indicate that sucrose, raffinose, and stachyose were degraded during APTS labeling in a way that exposed free reducing ends. We hypothesized that the α-1,β-2 -glycosidic linkage between glucose and fructose residues was the most labile linkage in sucrose, raffinose, and stachyose. Accordingly, the three peaks observed at 2.4, 3.0, and 3.8 glucose units on the overlaid electropherograms (Fig. 2) were assumed to be APTS-labeled glucose, melibiose, and manninotriose, respectively. Fructose, the other degradation product, formed two enantiomers of APTS-labeled fructose that appeared as two small peaks near the peak of the DP 2 bracket (labeled with a manufacturer-proprietary non-APTS fluorophore) as determined by analyzing a fructose standard (data not shown). Labeling of the degradation product of sucrose and raffinose was further verified by the matching glucose units of APTS-labeled glucose and melibiose standards, respectively (data not shown). Theoretically, any attempt to label non-reducing OS via reductive amination should not produce distinct electropherogram peaks due to the lack of available aldehyde groups, so this result was rather surprising. Importantly, sucrose, raffinose, and stachyose are ubiquitous and abundant in many plant foods, including legumes, peanuts, and tree nuts, and are often analyzed during routine analysis and quality control of food products. Therefore, one must consider that when analyzing OS (e.g., free OS, released N-glycans, and OS derived from polysaccharides) labeled via reductive amination in complex plant-derived samples, the peaks resulting from cleavage of non-reducing carbohydrates may lead to misidentification and inaccurate characterization/quantification. Hence, analysts should be aware of this issue when analyzing samples containing such susceptible OS. Whenever possible, the OS of interest should be separated from non-reducing carbohydrates before labeling, such as through gel filtration. In particular, for the analysis of N-glycans, protein precipitation or membrane filtration could be performed before releasing N-glycans in order to exclude non-reducing soluble carbohydrates.

3.2. Effect of acid on OS degradation during solvent evaporation at mild temperature

Graphitized carbon is the method of choice for desalting OS in food samples or biological matrices prior to analysis by LC-MS (Fig. 1B) [27,28]. Neutral and acidic OS can be sequentially eluted from a graphitized carbon column with acetonitrile-water mixtures and acetonitrile-water mixtures containing dilute TFA; they can also be directly eluted as a single fraction with acetonitrile-water mixtures containing dilute TFA [27,28]. Although lyophilization can fulfill the subsequent step of solvent removal, centrifugal evaporation is more frequently used as it is more affordable and time-efficient. In this study, we tested four standard OS, 6′-SLN and 3′-SL (milk OS) and raffinose and stachyose (legume OS), during solvent evaporation and discovered significant degradation. After drying the OS solutions at 37 °C to remove the solvent containing 0.1% TFA, LC-MS analysis revealed additional peaks in the chromatograms corresponding to degradation products (Fig. 3). The chromatogram of 6′-SLN displayed several additional peaks generated by

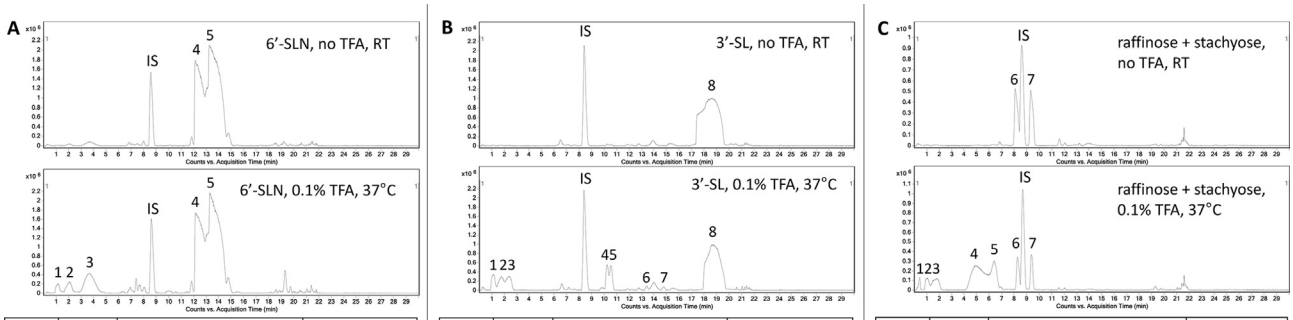

Peak no.	RT (min)	MS1 major peak m/z	Compound
1	1.1	**310.11**, 292.10, 619.22	Sialic acid
2	2.1	**384.15**, 366.14, 767.29	N-Acetyllactosamine
3	3.6	**384.15**, 366.14, 767.29	N-Acetyllactosamine
4	12.1	**675.25**	6′-SLN
5	13.4	**675.25**	6′-SLN

Peak no.	RT (min)	MS1 major peak m/z	(Suggested) compound
1	1.1	**310.11**, 619.22, 292.10	Sialic acid
2	1.8	685.24, 325.11, **343.12**, 163.06	Lactose
3	2.4	685.24, **343.12**, 325.11, 163.06	Lactose
4	10.2	**616.21**, 598.20	3′-SL lactone
5	10.5	**616.21**, 598.20	3′-SL lactone
6	13.4	598.20, **616.21**	3′-SL lactone
7	14.8	**616.21**, 598.20	3′-SL lactone
8	18.7	454.16, **634.22**, 292.10	3′-SL

Peak no.	RT (min)	MS1 major peak m/z	Compound
1	0.4	163.06, **325.11**	Fructose
2	1.1	163.06, 325.11, 685.24, 667.23, **343.12**	Melibiose
3	1.8	163.06, 325.11, 685.24, 667.23, **343.12**	Melibiose
4	5.0	487.17, 325.11, **505.18**, 163.06, 343.12	Manninotriose
5	6.4	487.17, 325.11, **505.18**, 163.06, 343.12	Manninotriose
6	8.1	325.11, 163.06, 343.12, 685.24, 847.29	Raffinose
7	9.4	505.18, 487.17, 325.11, 163.06, 343.12	Stachyose

Fig. 3. LC-Q-TOF base peak chromatograms of 6′-SLN (A), 3′-SL (B), and a mixture of raffinose and stachyose (C) prepared in 40% acetonitrile and dried at room temperature (no TFA, top chromatogram), and prepared in 40% acetonitrile containing 0.1% TFA and dried at 37 °C (bottom chromatogram). Xylosyl-cellobiose (internal standard, IS) was added to each sample at a concentration of 1 μg mL-1 before injection. The major peaks in the ESI mass spectra of each chromatographic peak are summarized in the tables (ranked by signal intensity from high to low) below each pair of chromatograms. The m/z values of the protonated molecules ($[M+H]^+$) are marked in bold.

degradation that were not present when 6′-SLN was dried in absence of acid at room temperature (Fig. 3A). The new peaks were confirmed by mass as 6′-SLN degradation products: N-acetylneuraminic acid (Neu5Ac, peak 1) and two anomers of N-acetyllactosamine (peaks 2 and 3). Similarly, Neu5Ac (peak 1) and two anomers of lactose (peaks 2 and 3) were identified in the chromatogram generated from 3′-SL dried in solvent containing 0.1% TFA (Fig. 3B). In addition to the products of desialylation, 3′-SL generated four additional peaks (peaks 4, 5, 6, and 7) when drying the OS in 40% acetonitrile with 0.1% TFA. These four peaks were all chiefly composed of a mixture of two ions with *m/z* 616.21 and 598.20, which could be the products of acid-catalyzed lactonization involving the carboxyl group on the Neu5Ac residue and one of the hydroxyl groups on galactose residue [29,30]. Degradation of 6′-SLN and 3′-SL was also evident in the abundance of each OS measured after solvent evaporation. To obtain the relative abundances of the OS dried under each set of conditions, the peak areas of each OS were first normalized against the peak area of the internal standard to compensate for differences in ionization efficiency. After normalizing against the internal standard, the samples were normalized against the data collected for the samples dried at room temperature in absence of TFA, which were considered the control group. In-source fragment ions and aggregate ions were merged with the protonated molecules ($[M+H]^+$) of the OS for peak area integration. More details about in-source fragmentation and aggregate ion formation are discussed in the next section. The relative abundances of 6′-SLN and 3′-SL standards that underwent evaporation in 40% acetonitrile with 0.1% TFA at 37 °C were 8.5% and 26.5% lower, respectively, than when dried at room temperature in the absence of TFA (Fig. 4A and B).

For raffinose and stachyose, the additional chromatographic peaks generated during the evaporation of 40% acetonitrile with 0.1% TFA (Fig. 3C) were tentatively identified as fructose (peak 1), two anomers of melibiose (peaks 2 and 3), and two anomers of manninotriose (peaks 4 and 5). Injecting raffinose and stachyose samples separately confirmed that peaks 2 and 3 were generated from raffinose, and peaks 4 and 5 were from stachyose. The monosaccharides composing raffinose and stachyose (fructose, glucose, and galactose) are all hexoses, and thus the resulting degradation products could not be unambiguously identified by mass spectrometry because the monosaccharides have identical masses. To verify our hypothesis that raffinose and stachyose generated melibiose and manninotriose during solvent evaporation, we conducted an enzymatic treatment using the enzyme invertase on raffinose and stachyose. The retention times of the enzymatically generated melibiose and manninotriose matched precisely the degradation products generated from raffinose and stachyose during solvent evaporation at 37 °C in the presence of TFA. The relative abundances of raffinose and stachyose were lower in the samples dried at 37 °C in presence of TFA compared with the samples without acid and/or dried at room temperature

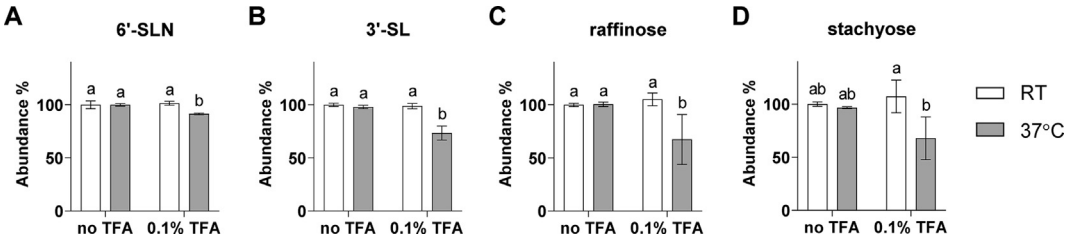

Fig. 4. Relative abundances of 3′-SL (A), 6′-SLN (B), raffinose (C), and stachyose (D) after evaporation of different solvents (40% acetonitrile with or without 0.1% TFA) at various temperatures (room temperature (RT) or 37 °C). Relative abundances were measured by LC-Q-TOF and are normalized to the samples dried in absence of TFA at room temperature. Data are presented as mean ± standard deviation (n = 3). Different letters on the bars indicate significant differences for each analyte among samples subjected to different treatments (p < 0.05 by Tukey's method).

(Fig. 4C and D). As there was no significant loss for any of the four OS when dried at room temperature in 40% acetonitrile with 0.1% TFA (Fig. 4A–D), we proposed that when removing solvents containing TFA from OS samples by centrifugal evaporation, no heating should be applied. While it is well known that concentrated TFA is often used for breaking down OS or polysaccharides at high temperatures for subsequent monosaccharide composition analysis [12,13], this work demonstrated that even minute TFA concentrations at mild temperatures can cause partial degradation of susceptible OS. Hence, this effect needs to be taken into account when using TFA, even dilute, in glycomic analysis.

3.3. Evaluating in-source fragmentation of OS in LC-MS analysis

When analyzing OS with LC-MS in the positive ion mode, in most cases, $[M+H]^+$ or $[M + H-H_2O]^+$ represent the major peaks in the ESI mass spectra. However, this study revealed significant in-source fragmentation for many OS, including a representative OS found in bovine milk (3′-SL) and two important OS (raffinose and stachyose) abundant in legumes (Fig. 5). The tallest peak in the ESI mass spectra of 3′-SL was *m/z* 454.16 ($[M-Hex-H_2O + H]^+$), followed by the peaks *m/z* 634.22 ($[M+H]^+$), *m/z* 292.10 (($[M-2Hex-H_2O + H]^+$ or $[Neu5Ac-H_2O + H]^+$), and *m/z* 1267.43 ($[2M + H]^+$) (Fig. 5A). By comparison, the MS1 spectra of raffinose and stachyose were even more complex. For raffinose, the most abundant peaks in the ESI mass spectra, ranked by signal intensity from high to low, were *m/z* 325.11, *m/z* 163.06, *m/z* 343.12, and *m/z* 685.24 (Fig. 5B). The theoretical *m/z* of protonated raffinose, 505.18 ($[M+H]^+$), was much less abundant than the other ions mentioned above. Similarly, the tallest peak in the ESI mass spectra of stachyose did not correspond to the $[M+H]^+$, but rather to its fragments. The most abundant MS1 ions of stachyose were *m/z* 505.18, *m/z* 487.17, and *m/z* 325.11, whereas the theoretical *m/z* of stachyose, 667.23 ($[M+H]^+$) and 649.22 ($[M-H_2O + H]^+$), were found in extremely low abundance (Fig. 5C). Therefore, if one were unaware of this potential for in-source fragmentation and were to make OS assignments only based on the observed ESI mass spectra, it is highly possible that a fragment of stachyose would be misannotated as an OS consisting of three hexose residues. Similar issues were also recently reported for LC-MS-based cellular metabolomics [31] and MS-based lipidomics [32].

In-source fragmentation of OS in LC-MS analysis is usually not severe and only slightly decreases the signal intensities of protonated molecules. However, we observed that the α-1,β-2 -glycosidic linkage between the glucose and fructose in raffinose and stachyose was extraordinarily labile compared with other common glycosidic linkages, similar to our prior observation with the APTS labeling in acid and solvent evaporation in presence of TFA at 37 °C. For the LC-MS analysis of raffinose, we suggest that the α-1,β-2 -glycosidic linkage was cleaved either at the electrospray ionization (ESI) stage or after ESI but before the ions entered the mass analyzer, thus abundant fructose (*m/z* 163.06) and melibiose (*m/z* 325.11 and *m/z* 343.12) were generated (Fig. 5B). Moreover, just after the fragmentation, two melibiose units formed an aggregate ion $[2M + H]^+$ to generate the peak at *m/z* 685.24. In the MS1 spectra of stachyose (Fig. 5C), the predominant peaks at *m/z* 505.18 and *m/z* 487.17 were identified as manninotriose, one of the two products of α-1,β-2 linkage cleavage from stachyose. The significant peak at *m/z* 325.11 indicated that in-source fragmentation also occurred on the α-1,6-glycosidic linkage in the middle of stachyose to generate OS containing two hexose residues, whereas the peaks at *m/z* 1171.40 and *m/z* 1009.35 indicated the occurrence of aggregate ion formation where stachyose-manninotriose aggregate ions and manninotriose-manninotriose aggregate ions, respectively, were formed. In-source fragmentation and aggregate ion formation have

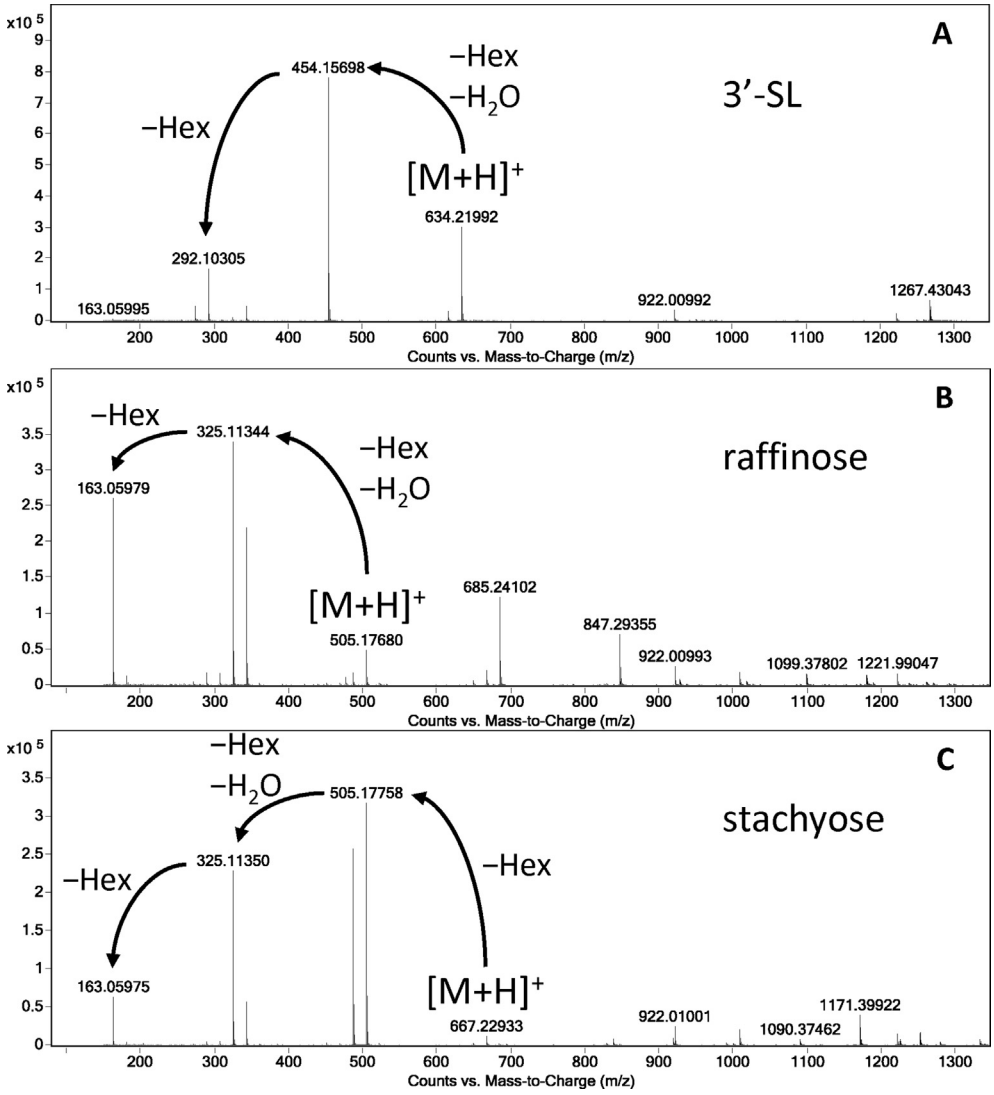

Fig. 5. LC-Q-TOF ESI mass spectra of standards of 3′-SL (A), raffinose (B), and stachyose (C) with extensive in-source fragmentation. Peaks 922.01 and 1221.99 are calibration ions.

occasionally been seen in the analysis of OS using ESI-MS [33–35], but to our knowledge, aggregate ion formation involving in-source fragmentation products was not reported previously. In previous studies employing LC-ESI-MS for the analysis of raffinose and stachyose, $[M+Na]^+$ (*m/z* 527 and *m/z* 689, respectively), $[M-H]^-$ (*m/z* 503 and *m/z* 665, respectively), or $[M + HCOO]^-$ (*m/z* 549 and *m/z* 771, respectively) were the most significant ions in the ESI mass spectra [36–38]. Because the OS ions in the current study were all protonated, we suspect that protonation, which was reported to facilitate glycosidic linkage fragmentation previously [39,40], contributed substantially to the cleavage of α-1,β-2 -glycosidic linkage in raffinose and stachyose.

Aggregate ion formation was also observed with melibiose and manninotriose, which formed aggregate ions of *m/z* 685.24 (Supporting information Fig. S1A and C) and *m/z* 1009.3446 (Supporting information Fig. S1B and D), respectively, in the ESI mass spectra. This further corroborated our hypothesis that the ions *m/z* 685.24 and *m/z* 1009.35 in the ESI mass spectra of raffinose and stachyose, respectively, were in reality aggregate ions formed by the in-source fragments.

To further confirm that the ions observed in the MS1 spectra originated from the same OS (3′-SL, raffinose, or stachyose), we extracted and overlaid the chromatograms of the major ions (Fig. 6). The retention times of all the major ions in the MS1 spectra of 3′-SL (*m/z* 454.16, *m/z* 634.22, *m/z* 292.10, *m/*

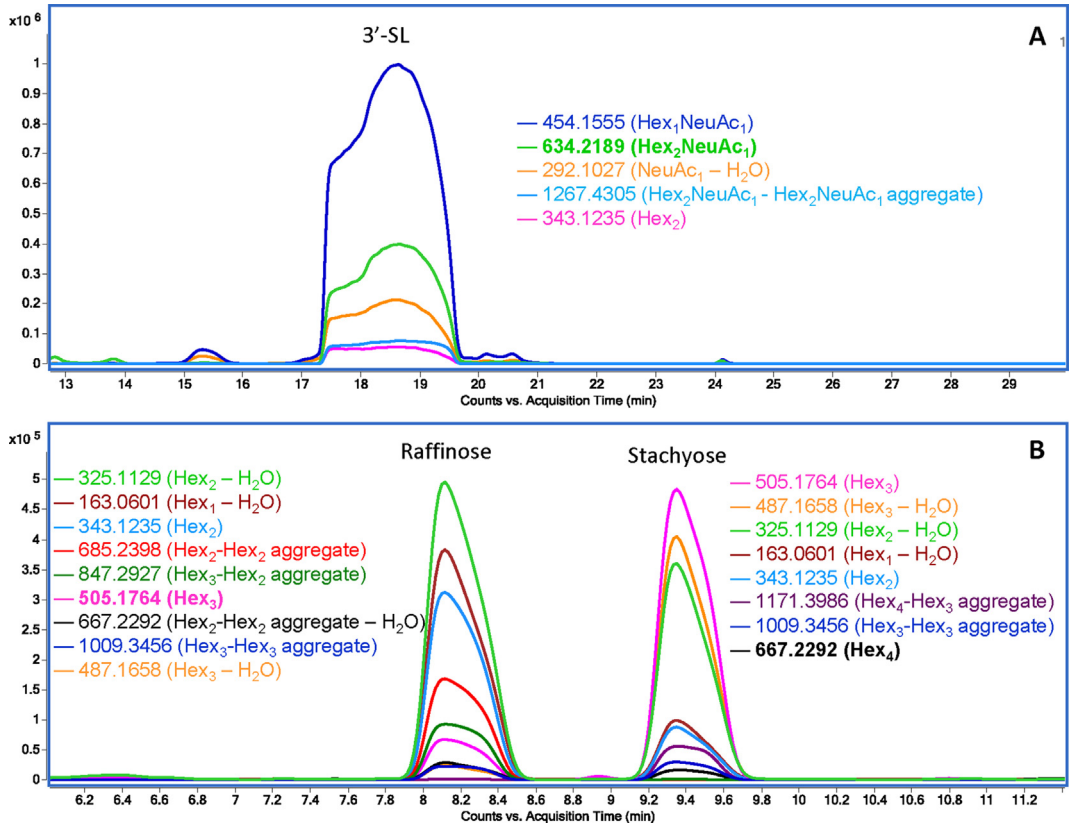

Fig. 6. Overlaid LC-Q-TOF chromatograms (EIC) of protonated molecules ($[M+H]^+$), in-source fragment ions, and aggregate ions of 3′-SL (A), and raffinose and stachyose (B). The m/z values of the protonated molecules are marked in bold. Hex: hexose. NeuAc: N-acetylneuraminic acid.

z 1267.43, and *m/z* 343.12), raffinose (*m/z* 325.11, *m/z* 163.06, *m/z* 343.12, *m/z* 685.24, *m/z* 847.29, *m/z* 505.18, *m/z* 667.23, *m/z* 1009.35, and *m/z* 487.17), and stachyose (*m/z* 505.18, *m/z* 487.17, *m/z* 325.11, *m/z* 163.06, *m/z* 343.12, *m/z* 1171.40, *m/z* 1009.35, and *m/z* 667.23), respectively, aligned correctly, providing evidence that those ions were indeed generated by in-source fragmentation and aggregate ion formation. The chromatographic peaks among different extracted-ion chromatograms (EIC) were also well aligned when the released N-glycans (Supporting information Fig. S2) and galactooligosaccharides were analyzed. Therefore, while analyzing real samples, overlaying the EIC of all identified OS could assist in identifying in-source fragment ions and prevent mis-annotation of the fragments as genuine OS [41].

3.4. Solutions for avoiding mis-annotation of in-source fragments as genuine OS in LC-MS analysis

The degree of in-source fragmentation can be affected by the capillary voltage, drying gas temperature, and numerous other parameters of the mass spectrometer. Despite adjusting those parameters, raffinose and stachyose still had extensive in-source fragmentation (data not shown). Although negative ion mode and permethylation may stabilize the labile sialylated OS (and are sometimes used) [42,43], analyzing OS in native forms in positive ion mode is still extensively done for both targeted and untargeted glycomics [24,44–46]. Even if the majority of OS may not be severely affected, being aware of the potential in-source fragmentation of particular OS and the consequential effects is crucial to correctly interpret the LC-MS data (Fig. 1B).

As mentioned above, protonated molecules were barely observed in the ESI mass spectra of some analytes, such as stachyose. Thus, correct assignment of OS identities (i.e., DP and monosaccharide composition) without performing a separate comparison with the corresponding standards would not be possible. In particular, when performing untargeted analysis for discovering novel OS in foods, it is usually not possible to tell whether the identified OS contain fragile linkages or whether a particular mass spectral peak represents a true OS or an in-source fragment. Therefore, it is crucial to find a strategy to deal with the potential incorrect

identifications that may result from extensive in-source fragmentation.

As we suspected protons would initiate in-source fragmentation of susceptible OS, we tried to replace formic acid with other mobile phase additives, such as ammonium acetate, to reduce the proton concentration and facilitate the formation of adducts other than protonated molecules. When a mobile phase containing 5 mM ammonium acetate was used, in-source fragmentation of raffinose and stachyose was greatly diminished (Fig. 7A and B). In their ESI mass spectra, ammonium adduct ions were the most intense peaks, and sodium and potassium adduct ions were also observed at lower intensities. For 3′-SL, in-source fragmentation was also reduced when changing the mobile phase additive from 0.1% formic acid to 5 mM ammonium acetate (Fig. 7C). However, the protonated form of 3′-SL was still more abundant than other adduct ions ($[M + NH_4]^+$, $[M+Na]^+$, and $[M+K]^+$), and there was still a considerable abundance of in-source fragment ions (*m/z* 454.16). The relative abundance of protonated molecules and the other adduct ions of different OS may be related to the specific OS molecule properties, such as elemental composition [47].

The enhanced stability of the ammonium and metal ion adducts was also revealed in their tandem-MS fragmentation behavior. For example, when using collision energy settings that were optimized for protonated carbohydrates, the abundance of the protonated raffinose precursor in its MS2 spectra was lower than the abundance of ammonium adduct ions in their MS2 spectra, and sodium and potassium adduct ions remained completely unfragmented (Supporting information Fig. S3). This confirmed that protonated ions were less stable and fragmented more easily compared

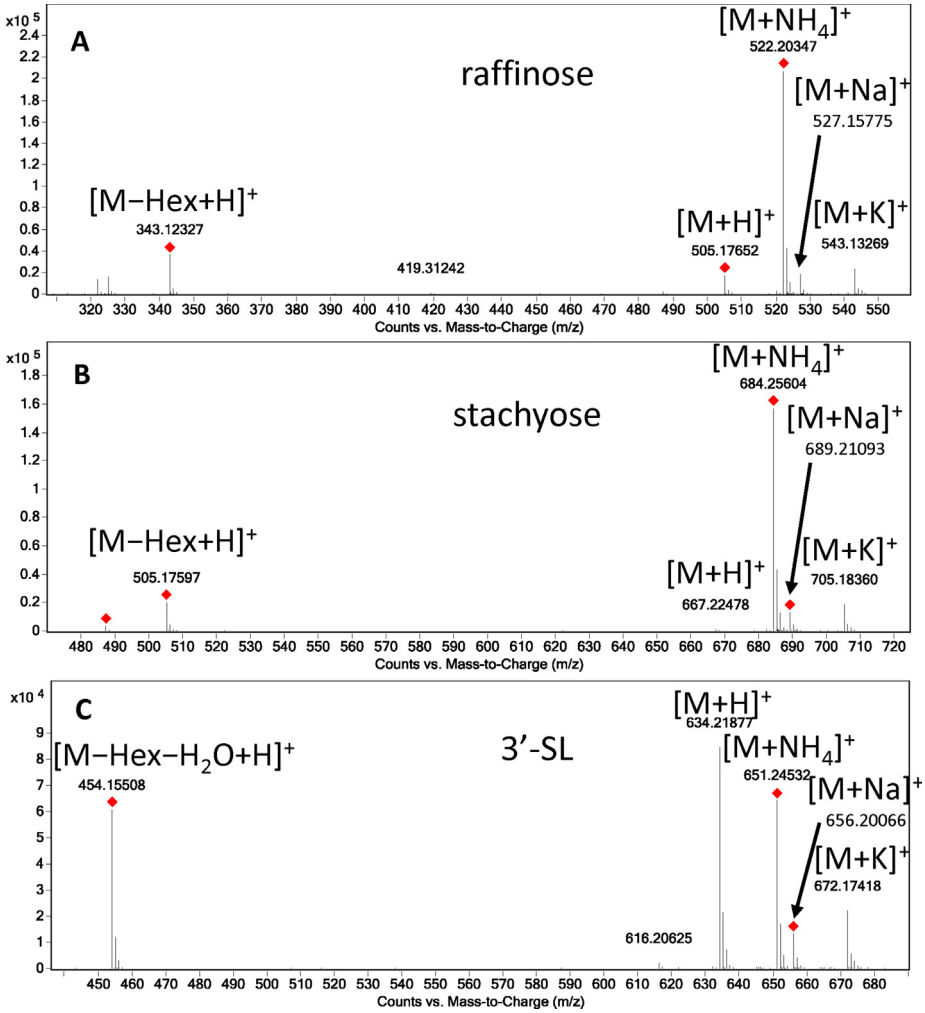

Fig. 7. LC-Q-TOF ESI mass spectra of raffinose (A), stachyose (B), and 3′-SL (C) run with a mobile phase containing 5 mM ammonium acetate in positive ion mode.

with the other adducts. An alkaline metal ion can coordinate with several oxygen atoms in an OS molecule and thus stabilize the adduct ions, while a proton can coordinate with at most two oxygen atoms [40]. Ammonium ions appear to behave similarly to alkaline metal ions, as the ammonium adducts were also more stable than the protonated molecules.

Here we identified a simple strategy that can reduce the probability of incorrect oligosaccharide identification resulting from extensive in-source fragmentation. In the ESI mass spectra of raffinose, stachyose, and 3′-SL analyzed with a mobile phase containing 5 mM ammonium acetate, the identity of the true intact analyte is evidenced by the existence of $[M + NH_4]^+$, $[M+Na]^+$, and $[M+K]^+$, while the in-source fragments did not produce these adducts. Therefore, when conducting untargeted analysis, the presence of these adduct ions in significant abundances would suggest the authenticity of the OS. In summary, modifying the mobile phase to prevent the formation of labile protonated molecules could reduce in-source fragmentation and, more importantly, ensure correct identification of susceptible OS.

4. Conclusions

This study demonstrates the susceptibility of specific OS linkages to degradation induced by heat and acid. In addition to the well-known susceptible linkages of sialylation, the α-1,β-2 linkages in sucrose, raffinose, and stachyose are also labile in an acidic environment. This degradation occurred not only at high temperatures in presence of concentrated acids but also at mild temperatures in the presence of dilute acids, as commonly used in OS purification workflows. Therefore, careful consideration must be given to ensure the accuracy of glycan characterization when acids are used at any step in a conventional glycomics workflow. This is especially important for samples containing OS consisting of sialyl linkages or α-1,β-2 glycosidic linkages. To eliminate the potential interference caused by the degradation products of non-reducing OS during labeling and analysis, it is advisable to fractionate such susceptible non-reducing sugars before labeling. The degradation of OS during centrifugal evaporation of native OS can be prevented by drying samples at room temperature. In-source fragmentation in LC-MS analysis under positive ion mode can be greatly diminished by changing the mobile phase additive from formic acid to ammonium acetate to reduce the formation of labile protonated molecules. Incorrect identification for the susceptible OS can be successfully avoided by distinguishing authentic OS from in-source fragment ions with the presence of ammonium, sodium, and potassium adduct ions.

Conflict of interest

The authors have declared no conflict of interest.

Acknowledgements

The authors thank Prozyme Inc. (now Agilent) for providing the APTS-labeling reagents and Gly-Q consumables. This study was funded by the U.S. Department of Agriculture's (USDA) Agricultural Marketing Service through grant AM170100XXXX-G011 and USDA NIFA Hatch grant CA-D-FST-2187-H. The content of this publication is solely the responsibility of the authors and does not necessarily represent the official views of the USDA. Yu-Ping Huang is a recipient of Yen Chuang Taiwan Fellowship.

Appendix.

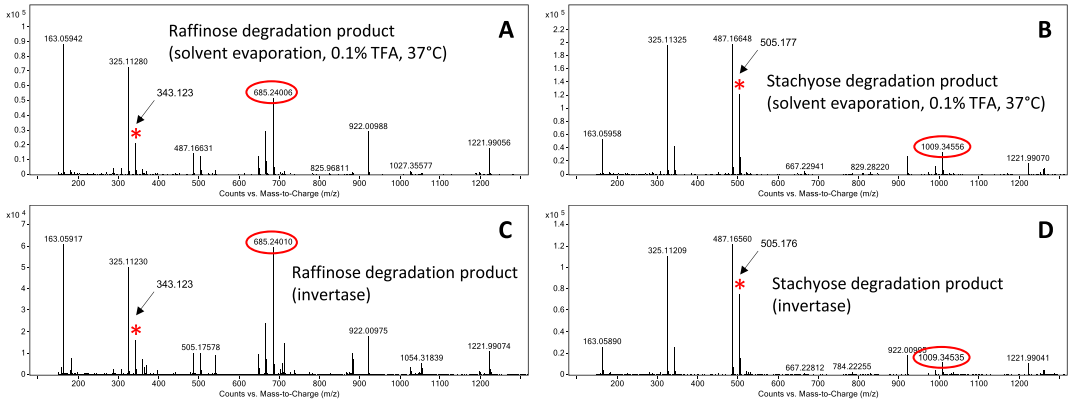

Fig. S1. LC-Q-TOF ESI mass spectra of degradation products at 1.8 min (A) and 6.4 min (B) generated from raffinose and stachyose, respectively, during solvent evaporation at 37 °C in the presence of TFA, and the spectra of melibiose (C) and manninotriose (D) generated through invertase enzymatic treatment of raffinose and stachyose, respectively. Peaks denoted by asterisks are the protonated molecules ($[M+H]^+$). The m/z values of aggregate ions are marked in red circles. Peaks 922.01 and 1221.99 are calibration ions.

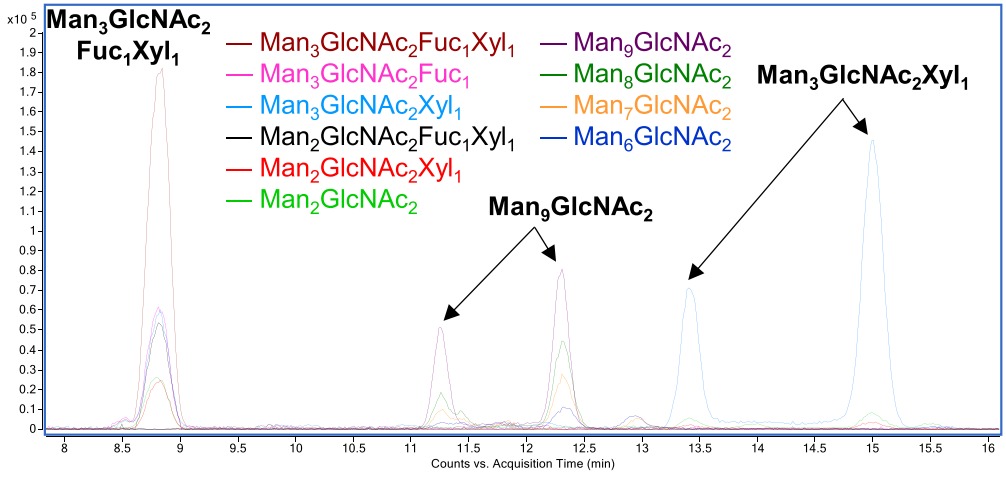

Fig. S2. Overlaid chromatograms (EIC) of protonated molecules and the corresponding in-source fragment ions of selected N-glycans ($Man_3GlcNAc_2Fuc_1Xyl_1$, $Man_9GlcNAc_2$, and $Man_3GlcNAc_2Xyl_1$) released from almond proteins. Man: mannose. GlcNAc: N-Acetylglucosamine. Fuc: fucose. Xyl: xylose.

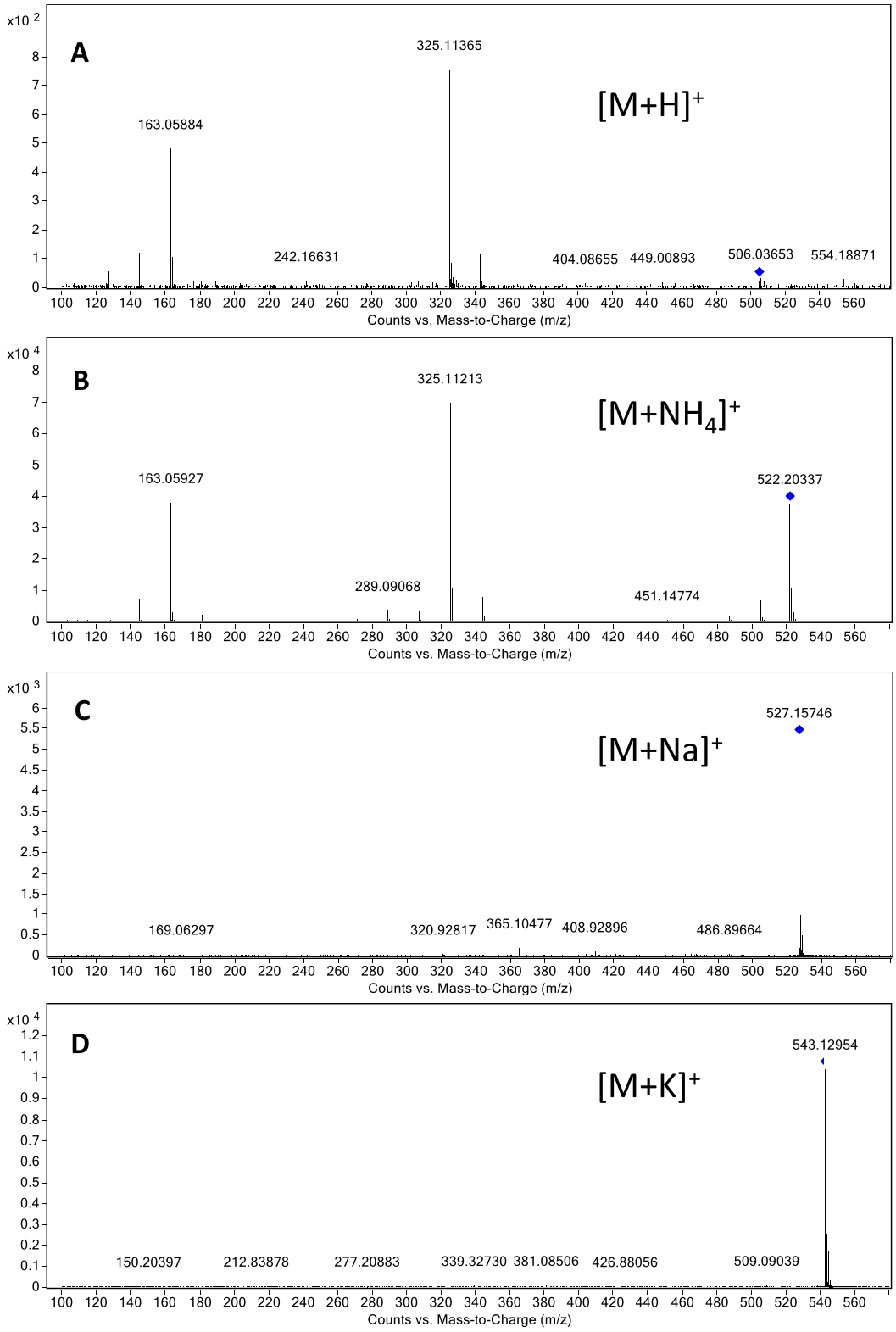

Fig. S3. LC-Q-TOF MS2 spectra of $[M+H]^+$ (collision energy 3.07 V; A), $[M + NH_4]^+$ (collision energy 3.29 V; B), $[M+Na]^+$ (collision energy 3.35 V; C), and $[M+K]^+$ (collision energy 3,56 V; D) of raffinose.

References

[1] Patel S, Goyal A. Functional oligosaccharides: production, properties and applications. World J Microbiol Biotechnol 2011;27:1119–28.

[2] Parc AL, Karav S, Leite Nobrega de Moura Bell JM, Frese SA, Liu Y, Mills DA, et al. A novel endo-β-N-acetylglucosaminidase releases specific N-glycans depending on different reaction conditions. Biotechnol Prog 2015;31:1323–30.

[3] Mussatto SI, Mancilha IM. Non-digestible oligosaccharides: a review. Carbohydr Polym 2007;68:587–97.

[4] Lai H-M, Huang Y-P. Effects of ball milling on the properties of colored rice bran. Gums Stab Food Indust 2014;17:155–63.

[5] Parajó JC, Garrote G, Cruz JM, Dominguez H. Production of xylooligosaccharides by autohydrolysis of lignocellulosic materials. Trends Food Sci Technol 2004;15:115–20.

[6] Xing H, Yaylayan VA. Mechanochemical depolymerization of inulin. Carbohydr Res 2018;460:14–8.

[7] Yuan X, Wang J, Yao H. Production of feruloyl oligosaccharides from wheat bran insoluble dietary fibre by xylanases from Bacillus subtilis. Food Chem 2006;95:484–92.

[8] Bunyatratchata A, Huang Y-P, Ozturk G, Cohen JL, Bhattacharya M, MLN de Moura Bell J, et al. Effects of industrial thermal treatments on the release of bovine colostrum glycoprotein N-glycans by endo-β-N-acetylglucosaminidase. J Agric Food Chem 2020;68:15208–15.

[9] Swennen K, Courtin CM, Delcour JA. Non-digestible oligosaccharides with prebiotic properties. Crit Rev Food Sci Nutr 2006;46:459–71.

[10] de Moura FA, Macagnan FT, da Silva LP. Oligosaccharide production by hydrolysis of polysaccharides: a review. Int J Food Sci 2015;50:275–81.

[11] Wang S, Copeland L. Effect of acid hydrolysis on starch structure and functionality: a review. Crit Rev Food Sci Nutr 2015;55:1081–97.

[12] Shi H, Wan Y, Li O, Zhang X, Xie M, Nie S, et al. Two-step hydrolysis method for monosaccharide composition analysis of natural polysaccharides rich in uronic acids. Food Hydrocoll 2020;101:105524.

[13] Tabarsa M, You S, Dabaghian EH, Surayot U. Water-soluble polysaccharides from Ulva intestinalis: molecular properties, structural elucidation and immunomodulatory activities. J Food Drug Anal 2018;26:599–608.

[14] Miller RL, Guimond SE, Prescott M, Turnbull JE, Karlsson N. Versatile separation and analysis of heparan sulfate oligosaccharides using graphitized carbon liquid chromatography and electrospray mass spectrometry. Anal Chem 2017;89: 8942–50.

[15] Lamari FN, Kuhn R, Karamanos NK. Derivatization of carbohydrates for chromatographic, electrophoretic and mass spectrometric structure analysis. J Chromatogr B 2003;793: 15–36.

[16] Ruhaak LR, Xu G, Li Q, Goonatilleke E, Lebrilla CB. Mass spectrometry approaches to glycomic and glycoproteomic analyses. Chem Rev 2018;118:7886–930.

[17] Aich U, Hurum DC, Basumallick L, Rao S, Pohl C, Rohrer JS, et al. Evaluation of desialylation during 2-amino benzamide labeling of asparagine-linked oligosaccharides. Anal Biochem 2014;458:27–36.

[18] Bigge JC, Patel TP, Bruce JA, Goulding PN, Charles SM, Parekh RB. Nonselective and efficient fluorescent labeling of glycans using 2-amino benzamide and anthranilic acid. Anal Biochem 1995;230:229–38.

[19] Evangelista RA, Chen F-TA, Guttman A. Reductive amination of N-linked oligosaccharides using organic acid catalysts. J Chromatogr A 1996;745:273–80.

[20] Albrecht S, Schols HA, van Zoeren D, van Lingen RA, Groot Jebbink LJM, van den Heuvel EGHM, et al. Oligosaccharides in feces of breast- and formula-fed babies. Carbohydr Res 2011;346:2173–81.

[21] Galeotti F, Coppa GV, Zampini L, Maccari F, Galeazzi T, Padella L, et al. Capillary electrophoresis separation of human milk neutral and acidic oligosaccharides derivatized with 2-aminoacridone. Electrophoresis 2014;35:811–8.

[22] Lorenz D, Erasmy N, Akil Y, Saake B. A new method for the quantification of monosaccharides, uronic acids and oligosaccharides in partially hydrolyzed xylans by HPAEC-UV/VIS. Carbohydr Polym 2016;140:181–7.

[23] Ruhaak LR, Steenvoorden E, Koeleman CAM, Deelder AM, Wuhrer M. 2-Picoline-borane: a non-toxic reducing agent for oligosaccharide labeling by reductive amination. Proteomics 2010;10:2330–6.

[24] Aldredge DL, Geronimo MR, Hua S, Nwosu CC, Lebrilla CB, Barile D. Annotation and structural elucidation of bovine milk oligosaccharides and determination of novel fucosylated structures. Glycobiology 2013;23:664–76.

[25] Karav S, Parc AL, de Bell JMLNM, Frese SA, Kirmiz N, Block DE, et al. Oligosaccharides released from milk glycoproteins are selective growth substrates for infant-associated bifidobacteria. Appl Environ Microbiol 2016;82:3622–30.

[26] Tian T, Freeman S, Corey M, German JB, Barile D. Chemical characterization of potentially prebiotic oligosaccharides in brewed coffee and spent coffee grounds. J Agric Food Chem 2017;65:2784–92.

[27] Packer NH, Lawson MA, Jardine DR, Redmond JW. A general approach to desalting oligosaccharides released from glycoproteins. Glycoconj J 1998;15:737–47.

[28] Robinson RC, Colet E, Tian T, Poulsen NA, Barile D. An improved method for the purification of milk oligosaccharides by graphitised carbon-solid phase extraction. Int Dairy J 2018;80:62–8.

[29] Perreault H, Costello CE. Stereochemical effects on the mass spectrometric behavior of native and derivatized trisaccharide isomers: comparisons with results from molecular modeling. J Mass Spectrom 1999;34:184–97.

[30] Yu RK, Koerner TAW, Ando S, Yohe HC, Prestegard JH. High-resolution proton NMR studies of gangliosides. J Biochem 1985;98:1367–73.

[31] Xu Y-F, Lu W, Rabinowitz JD. Avoiding misannotation of in-source fragmentation products as cellular metabolites in liquid chromatography–mass spectrometry-based metabolomics. Anal Chem 2015;87:2273–81.

[32] Hu C, Luo W, Xu J, Han X. Recognition and avoidance of ion source-generated artifacts in lipidomics analysis. Mass Spectrom Rev 2021 (In press).

[33] Levin DS, Vouros P, Miller RA, Nazarov EG. Using a nanoelectrospray-differential mobility spectrometer-mass spectrometer system for the analysis of oligosaccharides with solvent selected control over ESI aggregate ion formation. J Am Soc Mass Spectrom 2007;18:502–11.

[34] Puppala M, Ponder J, Suryanarayana P, Reddy GB, Petrash JM, LaBarbera DV. The isolation and characterization of β-glucogallin as a novel aldose reductase inhibitor from emblica officinalis. PLoS One 2012;7:e31399.

[35] Séveno M, Cabrera G, Triguero A, Burel C, Leprince J, Rihouey C, et al. Plant N-glycan profiling of minute amounts of material. Anal Biochem 2008;379:66–72.

[36] Antonio C, Larson T, Gilday A, Graham I, Bergström E, Thomas-Oates J. Hydrophilic interaction chromatography/electrospray mass spectrometry analysis of carbohydrate-related metabolites from Arabidopsis thaliana leaf tissue. Rapid Commun Mass Spectrom 2008;22:1399–407.

[37] Liu M-H, Tong X, Wang J-X, Zou W, Cao H, Su W-W. Rapid separation and identification of multiple constituents in traditional Chinese medicine formula Shenqi Fuzheng Injection by ultra-fast liquid chromatography combined with quadrupole-time-of-flight mass spectrometry. J Pharm Biomed Anal 2013;74:141–55.

[38] Jorge TF, Florêncio MH, Ribeiro-Barros AI, António C. Quantification and structural characterization of raffinose family oligosaccharides in Casuarina glauca plant tissues by

porous graphitic carbon electrospray quadrupole ion trap mass spectrometry. Int J Mass Spectrom 2017;413:127–34.
[39] Ngoka LC, Gal JFrancois, Lebrilla CB. Effects of cations and charge types on the metastable decay rates of oligosaccharides. Anal Chem 1994;66:692–8.
[40] Cancilla MT, Penn SG, Carroll JA, Lebrilla CB. Coordination of alkali metals to oligosaccharides dictates fragmentation behavior in matrix assisted laser desorption ionization/fourier transform mass spectrometry. J Am Chem Soc 1996;118:6736–45.
[41] Song T, Aldredge D, Lebrilla CB. A method for in-depth structural annotation of human serum glycans that yields biological variations. Anal Chem 2015;87:7754–62.
[42] Dong X, Zhou S, Mechref Y. LC-MS/MS analysis of permethylated free oligosaccharides and N-glycans derived from human, bovine, and goat milk samples. Electrophoresis 2016;37:1532–48.
[43] Karlsson NG, Wilson NL, Wirth H-J, Dawes P, Joshi H, Packer NH. Negative ion graphitised carbon nano-liquid chromatography/mass spectrometry increases sensitivity for glycoprotein oligosaccharide analysis. Rapid Commun Mass Spectrom 2004;18:2282–92.
[44] Ruhaak LR, Deelder AM, Wuhrer M. Oligosaccharide analysis by graphitized carbon liquid chromatography–mass spectrometry. Anal Bioanal Chem 2009;394:163–74.
[45] Amicucci MJ, Nandita E, Galermo AG, Castillo JJ, Chen S, Park D, et al. A nonenzymatic method for cleaving polysaccharides to yield oligosaccharides for structural analysis. Nat Commun 2020;11:3963.
[46] Cho BG, Peng W, Mechref Y. Separation of permethylated O-glycans, free oligosaccharides, and glycosphingolipid-glycans using porous graphitized carbon (PGC) column. Metabolites 2020;10:433.
[47] Sugimura N, Furuya A, Yatsu T, Igarashi Y, Aoyama R, Izutani C, et al. Observed adducts on positive mode direct analysis in real time mass spectrometry – proton/ammonium adduct selectivities of 600-sample in-house chemical library. Eur J Mass Spectrom 2017;23:4–10.